Figure 1.

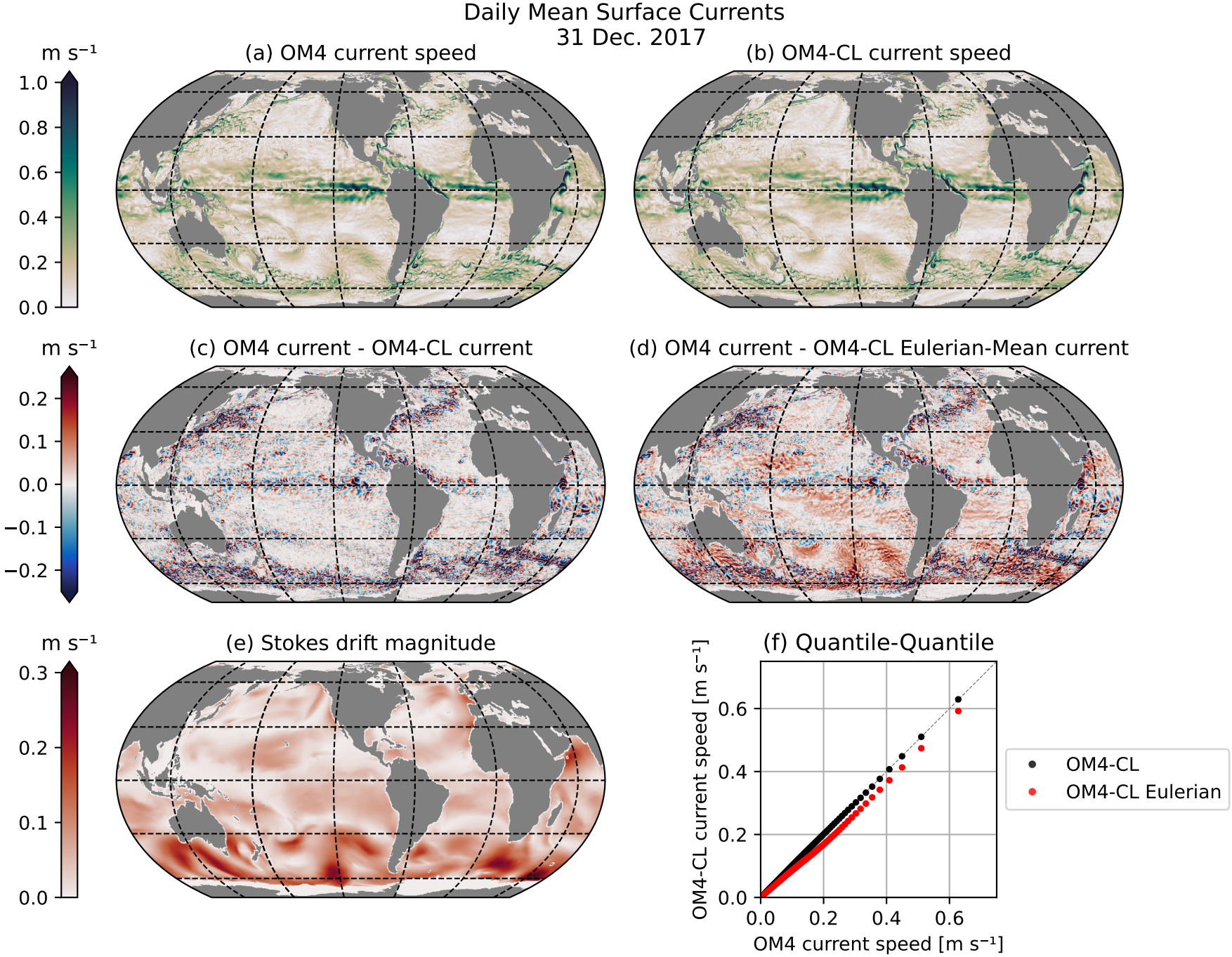
Daily Mean Surface Currents
31 Dec. 2017
m s⁻¹
(a) OM4 current speed
(b) OM4-CL current speed
(c) OM4 current - OM4-CL current
(d) OM4 current - OM4-CL Eulerian-Mean current
(e) Stokes drift magnitude
(f) Quantile-Quantile
OM4-CL current speed [m s⁻¹]
OM4 current speed [m s⁻¹]
OM4-CL
OM4-CL Eulerian

Figure 2.

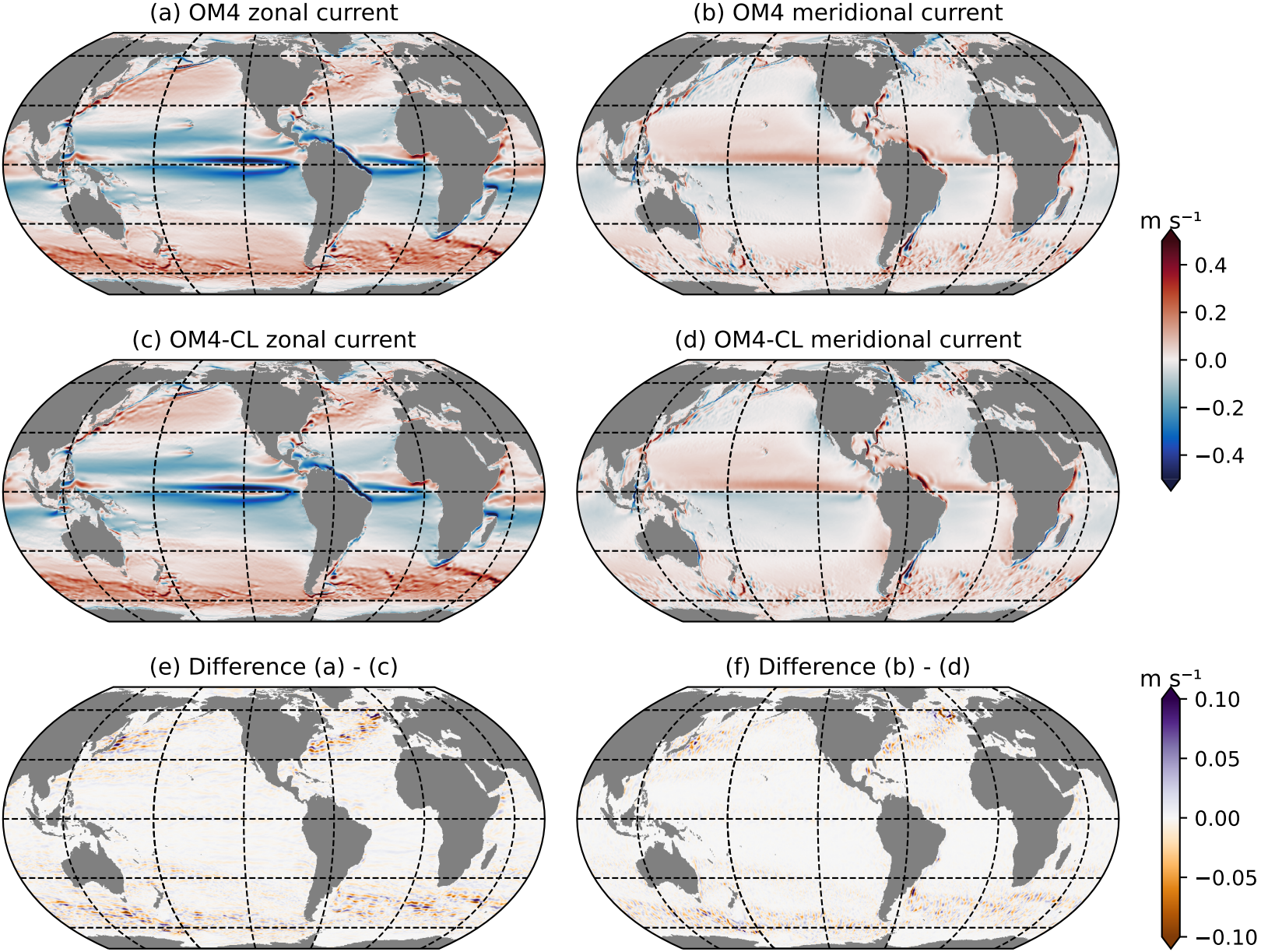
(a) OM4 zonal current
(b) OM4 meridional current
(c) OM4-CL zonal current
(d) OM4-CL meridional current
(e) Difference (a) - (c)
(f) Difference (b) - (d)
m s⁻¹
0.4
0.2
0.0
−0.2
−0.4
m s⁻¹
0.10
0.05
0.00
−0.05
−0.10

Figure 3.

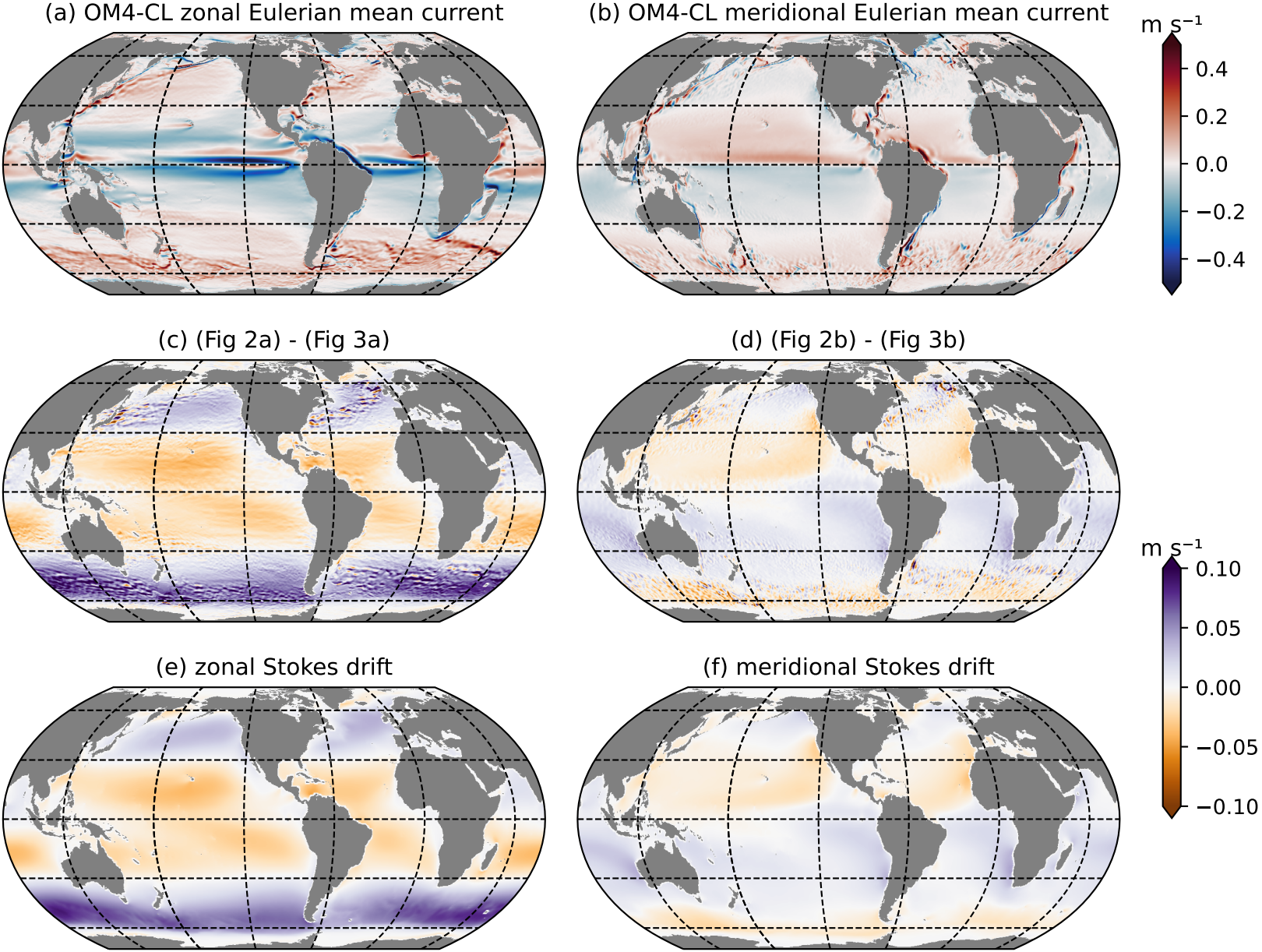
(a) OM4-CL zonal Eulerian mean current
(b) OM4-CL meridional Eulerian mean current
m s⁻¹
0.4
0.2
0.0
−0.2
−0.4
(c) (Fig 2a) - (Fig 3a)
(d) (Fig 2b) - (Fig 3b)
m s⁻¹
0.10
0.05
0.00
−0.05
−0.10
(e) zonal Stokes drift
(f) meridional Stokes drift

Stokes drift should not be added to ocean general circulation model velocities

Gregory L. Wagner[1], Navid C. Constantinou[2], and Brandon G. Reichl[3]

[1]Earth, Atmospheric, and Planetary Sciences, Massachusetts Institute of Technology, Cambridge, MA, USA
[2]Research School of Earth Sciences & ARC Centre of Excellence for Climate Extremes, Australian National University, Canberra, ACT, Australia
[3]NOAA Geophysical Fluid Dynamics Laboratory, Princeton, NJ, USA

Key Points:

- Adding Stokes drift to ocean general circulation model velocities is inconsistent with the wave-averaged Craik-Leibovich equations
- General circulation models with surface velocities primarily in geostrophic balance and *without* surface wave effects can simulate total Lagrangian-mean currents

Abstract

Studies of ocean surface transport often invoke the "Eulerian-mean hypothesis': that wave-agnostic general circulation models neglecting explicit surface waves effects simulate the Eulerian-mean ocean velocity time-averaged over surface wave oscillations. Acceptance of the Eulerian-mean hypothesis motivates reconstructing the total, Lagrangian-mean surface velocity by *adding* Stokes drift to model output. Here, we show that the Eulerian-mean hypothesis is inconsistent, because wave-agnostic models cannot accurately simulate the Eulerian-mean velocity if Stokes drift is significant compared to the Eulerian-mean or Lagrangian-mean velocity. We conclude that Stokes drift should not be added to ocean general circulation model output. We additionally show the viability of the alternative "Lagrangian-mean hypothesis" using a theoretical argument and by comparing a wave-agnostic global ocean simulation with an explicitly wave-averaged simulation. We find that our wave-agnostic model accurately simulates the Lagrangian-mean velocity even though the Stokes drift is significant.

Plain language summary

Physical oceanographers are taught that surface waves "induce" a time-averaged current called the Stokes drift. This notion motivates studies in which the total ocean surface transport of things like trash, oil, and kelp is estimated by the combined effect of "ocean currents" as simulated by an ocean model, or estimated from observations, and an *additional* "surface wave Stokes drift". In this paper, we show that ocean models and observations likely estimate total ocean transport *including* Stokes drift. So, we shouldn't "add Stokes drift" to model output or certain kinds of observations.

1 Introduction

Ocean surface waves complicate observations and models of near-surface ocean transport. Surface waves are associated with significant, yet oscillatory fluid displacements that must be time-averaged away to reveal the underlying persistent circulation. But time-averaging over surface waves is not straightforward: the ocean velocity averaged at a fixed position — the "Eulerian-mean velocity" — is missing a component of the total transport called the "Stokes drift" (Stokes, 1847). The total mean velocity responsible for advecting tracers, particles,

Corresponding author: Gregory L. Wagner, gregory.leclaire.wagner@gmail.com

and water parcels is called the "Lagrangian-mean velocity", because it can be obtained by time-averaging currents in a semi-Lagrangian reference frame that follows surface wave oscillations. These statements are summarized by the timeless formula

$$\boldsymbol{u}^{\mathrm{L}} = \boldsymbol{u}^{\mathrm{E}} + \boldsymbol{u}^{\mathrm{S}}\,, \tag{1}$$

where $\boldsymbol{u}^{\mathrm{L}}$ is the surface-wave-averaged Lagrangian-mean velocity, $\boldsymbol{u}^{\mathrm{E}}$ is the surface-wave-averaged Eulerian-mean velocity, and $\boldsymbol{u}^{\mathrm{S}}$ is the surface wave Stokes drift (Longuet-Higgins, 1969). On average, tracers, particles, and water parcels follow streamlines traced by Lagrangian-mean velocity $\boldsymbol{u}^{\mathrm{L}}$. (Formulas analogous to (1) also apply to velocities averaged over longer time intervals, such as supermonthly timescales over mesoscale ocean turbulence, but we do not discuss "other" Lagrangian-mean velocities in this paper.)

Most general circulation models of ocean transport and many observation-based estimates based on dynamical balances neither resolve surface wave oscillations nor invoke an explicit dependence on the surface wave state. Such "wave-agnostic" estimates should be *interpreted* as somehow time-averaged over surface wave oscillations. Note that the expression "wave-agnostic" excludes observations based on explicit averaging, such as moored Eulerian velocity measurements, or fully Lagrangian drifter or tracer-based estimates (for in depth discussions and examples see Longuet-Higgins, 1969; Middleton & Loder, 1989; Smith, 2006), that lack the ambiguity inherent to wave-agnosticism. We ask: do wave-agnostic models estimate the Eulerian-mean velocity, or the Lagrangian-mean velocity?

Studies investigating surface wave effects on ocean transport (Kubota, 1994; Tamura et al., 2012; Fraser et al., 2018; Iwasaki et al., 2017; Van den Bremer & Breivik, 2017; Dobler et al., 2019; Onink et al., 2019; Kerpen et al., 2020; Van Sebille et al., 2020; Bosi et al., 2021; Van Sebille et al., 2021; Durgadoo et al., 2021; Cunningham et al., 2022; Chassignet et al., 2021; Onink et al., 2022; Herman & Węsławski, 2022) often assume both the Stokes drift makes a significant contribution to total ocean surface transport, and that wave-agnostic models and observational products estimate the Eulerian-mean velocity. We call these assumptions the "Eulerian-mean hypothesis". Within the context of the Eulerian-mean hypothesis, the total Lagrangian-mean transport is constructed by adding an estimate of the Stokes drift velocity (derived from an estimate of the surface wave state) to model output or observational products, according to (1).

In this paper we argue that the Eulerian-mean hypothesis is inconsistent, in that its two components — accurate Eulerian-mean wave-agnostic simulations, in the presence of significant Stokes drift — are incompatible. Our argument, developed in section 2.1, uses a scaling analysis of the explicitly-wave-averaged Eulerian-mean Boussinesq equation (Craik & Leibovich, 1976; Huang, 1979). Because the Eulerian-mean hypothesis is internally inconsistent, ocean transport studies based on wave-agnostic model output or observations based on dynamical balances should not "add Stokes drift" to construct the total Lagrangian-mean transport.

To resolve the status of wave-agnostic models, we propose the alternative "Lagrangian-mean hypothesis", which supposes that wave-agnostic models estimate the Lagrangian-mean velocity. The Lagrangian-mean hypothesis is consistent in that it does not contain mutually incompatible components, and is therefore the only viable interpretation of wave-agnostic model output. The consistency of the Lagrangian-mean hypothesis does not, however, guarantee its *accuracy*. For example, wave-agnostic and explicitly wave-averaged large eddy simulations at meter scales exhibit dramatic, well-documented differences known as "Langmuir turbulence" (Skyllingstad & Denbo, 1995; McWilliams et al., 1997; Sullivan & McWilliams, 2010). We therefore turn to the question of whether wave-agnostic general circulation models — with scales much larger than the scales of large eddy simulation — provide accurate approximations of Lagrangian-mean general circulation models in section 2.2. Using a scaling argument, we predict that for *geostrophic* flows, surface wave terms in the Lagrangian-mean wave-averaged equations are negligible. This suggest that, at mesoscales and larger, the wave-

agnostic equations accurately approximate the Lagrangian-mean wave-averaged equations and the Lagrangian-mean hypothesis may hold.

We test the Lagrangian-mean hypothesis in section 3 by comparing output from a wave-agnostic "control" general circulation ocean model simulation with $1/4^\circ$ resolution that neglects surface wave effects on velocity and tracers with a "wave-averaged" general circulation ocean model simulation that explicitly includes surface waves. We find that the velocity in the wave-agnostic simulation is almost identical to the Lagrangian-mean velocity in the wave-averaged simulation. In section 4, we discuss the implications of our results for surface boundary layer parameterizations and the potential uses of wave-averaged general circulation models.

The success of the Lagrangian-mean hypothesis — even in a limited context — cannot be reconciled with the notion that Stokes drift is "wave-induced transport". This underlines the importance of regarding the total Lagrangian-mean momentum as the fundamental momentum variable, rather than the Eulerian-mean momentum. In such a paradigm, surface waves play no *direct* role in transport, and affect mean dynamics only through wave-averaged forces in the Lagrangian-mean momentum equation that are negligible at large oceanic scales.

2 Wave-averaged and wave-agnostic dynamics

The wave-averaged Craik–Leibovich Boussinesq momentum equation (Craik & Leibovich, 1976; Huang, 1979) can be written either in terms of the Eulerian-mean velocity $\boldsymbol{u}^{\mathrm{E}}$,

$$\partial_t \boldsymbol{u}^{\mathrm{E}} + \left(\boldsymbol{u}^{\mathrm{E}} \cdot \boldsymbol{\nabla}\right) \boldsymbol{u}^{\mathrm{E}} + f\,\hat{\boldsymbol{z}} \times \left(\boldsymbol{u}^{\mathrm{E}} + \boldsymbol{u}^{\mathrm{S}}\right) + \boldsymbol{\nabla}\left(\bar{p} + \tfrac{1}{2}\boldsymbol{u}^{\mathrm{S}} \cdot \boldsymbol{u}^{\mathrm{S}} + \boldsymbol{u}^{\mathrm{S}} \cdot \boldsymbol{u}^{\mathrm{E}}\right) = \bar{b}\,\hat{\boldsymbol{z}} + \boldsymbol{\mathcal{X}} + \boldsymbol{u}^{\mathrm{S}} \times \left(\boldsymbol{\nabla} \times \boldsymbol{u}^{\mathrm{E}}\right), \tag{2}$$

or the Lagrangian mean velocity, $\boldsymbol{u}^{\mathrm{L}}$,

$$\partial_t \boldsymbol{u}^{\mathrm{L}} + \left(\boldsymbol{u}^{\mathrm{L}} \cdot \boldsymbol{\nabla}\right) \boldsymbol{u}^{\mathrm{L}} + \left(f\,\hat{\boldsymbol{z}} - \boldsymbol{\nabla} \times \boldsymbol{u}^{\mathrm{S}}\right) \times \boldsymbol{u}^{\mathrm{L}} + \boldsymbol{\nabla}\bar{p} = \bar{b}\,\hat{\boldsymbol{z}} + \boldsymbol{\mathcal{X}} + \partial_t \boldsymbol{u}^{\mathrm{S}}\,. \tag{3}$$

In (2)–(3), $\bar{p}$ is the Eulerian-mean kinematic pressure (pressure scaled with ocean's reference density), $\bar{b} \overset{\text{def}}{=} -g\rho'/\rho_0$ is the Eulerian-mean buoyancy defined in terms of gravitational acceleration g, reference density ρ_0, and the Eulerian-mean density perturbation ρ', f is the Coriolis parameter, and $\hat{\boldsymbol{z}}$ is the unit vector pointing up. $\boldsymbol{\mathcal{X}}$ parametrizes subgrid momentum flux divergences associated with, for example, ocean surface boundary layer turbulence. We discuss $\boldsymbol{\mathcal{X}}$ further in section 4. Equations (2)–(3) are related by (1) and standard vector identities. Physical interpretations for the green surface wave terms in equations (2)–(3) are discussed by Wagner et al. (2021) in their section 2.1, Bühler (2014) in their section 11.3.2, and by Suzuki and Fox-Kemper (2016).

The green surface wave terms in equations (2) and (3) depend *explicitly* on the Stokes drift $\boldsymbol{u}^{\mathrm{S}}$ and therefore the surface wave state. The green terms distinguish equations (2)–(3) from the wave-agnostic Boussinesq momentum equation,

$$\partial_t \boldsymbol{u} + \left(\boldsymbol{u} \cdot \boldsymbol{\nabla}\right) \boldsymbol{u} + f\,\hat{\boldsymbol{z}} \times \boldsymbol{u} + \boldsymbol{\nabla} p = b\,\hat{\boldsymbol{z}} + \boldsymbol{\mathcal{X}}\,, \tag{4}$$

solved by typical, wave-agnostic ocean general circulation models.

2.1 The Eulerian-mean hypothesis is inconsistent

The Eulerian-mean hypothesis posits that velocities $\boldsymbol{u}$ that solve equation (4) are identical or similar to $\boldsymbol{u}^{\mathrm{E}}$ in (2) at ocean mesoscales and larger. The Eulerian-mean hypothesis therefore requires that (4) is a good approximation to (2) when $\boldsymbol{u}^{\mathrm{S}} \sim \boldsymbol{u}^{\mathrm{E}}$.

The central flaw in the Eulerian-mean hypothesis is that Stokes-Coriolis term $f\,\hat{\boldsymbol{z}} \times \boldsymbol{u}^{\mathrm{S}}$ in (2) is the same magnitude as the "Eulerian-mean component of the Coriolis force", $f\,\hat{\boldsymbol{z}} \times \boldsymbol{u}^{\mathrm{E}}$

when $\boldsymbol{u}^{\rm S} \sim \boldsymbol{u}^{\rm E}$. Thus for dynamics close to geostrophic and Ekman balance, (2) is not a good approximation to (4) because it does not represent the *total* Coriolis force $f\,\hat{\boldsymbol{z}} \times \boldsymbol{u}^{\rm L}$. Note that the Lagrangian-mean nature of the surface-wave-averaged Coriolis force, Ekman balance, and geostrophic balance is known (McWilliams & Restrepo, 1999; Samelson, 2022) and is also feature of internal-wave-averaged quasi-geostrophic dynamics (Wagner & Young, 2015; Kafiabad et al., 2021). Because Coriolis force acts on the Lagrangian-mean velocities, the only consistent interpretation of observations based on Ekman balance, like Johannessen et al. (2016), is that they estimate the Lagrangian-mean velocity. We finally note that a similar inconsistency in the Eulerian-mean hypothesis applies to tracer advection by $\boldsymbol{u}^{\rm L}$: $\boldsymbol{u}^{\rm E} \cdot \boldsymbol{\nabla} c$ is not a close approximation to $\boldsymbol{u}^{\rm L} \cdot \boldsymbol{\nabla} c$ when $\boldsymbol{u}^{\rm S} \sim \boldsymbol{u}^{\rm E}$.

The failure of the Eulerian-mean hypothesis to account for both tracer advection and the total Coriolis force is sufficient motivation to pursue the Lagrangian-mean hypothesis, and convinced readers may skip to section 2.2. The remainder of this section shows that the "vortex force" $\boldsymbol{u}^{\rm S} \times \big(\boldsymbol{\nabla} \times \boldsymbol{u}^{\rm E}\big)$ and "Stokes-Bernoulli" terms aside the pressure in (2) are $O(\mathrm{Ro})$, where

$$\mathrm{Ro} \stackrel{\rm def}{=} \frac{U}{fL}\,, \tag{5}$$

is the Rossby number for flows with velocity scale $|\boldsymbol{u}^{\rm L}| \sim |\boldsymbol{u}^{\rm S}| \sim |\boldsymbol{u}^{\rm E}| \sim U$ and horizontal scales $L \sim U/|\boldsymbol{\nabla}_h \boldsymbol{u}|$. We take U and L to apply to both mean currents and Stokes drift. Ro is typically less than unity for oceanic motion at mesoscales and larger.

Under slowly-modulated surface waves, the ratio

$$\frac{|\boldsymbol{\nabla}_h \boldsymbol{u}^{\rm S}|}{|\partial_z \boldsymbol{u}^{\rm S}|} \sim \frac{H}{L}\,, \tag{6}$$

is small, where H is the vertical decay scale of the Stokes drift. The approximation (6) simplifies the vortex force in (2) to

$$\boldsymbol{u}^{\rm S} \times (\boldsymbol{\nabla} \times \boldsymbol{u}^{\rm E}) \approx v^{\rm S}(\partial_x v^{\rm E} - \partial_y u^{\rm E})\,\hat{\boldsymbol{x}} - u^{\rm E}(\partial_x v^{\rm E} - \partial_y u^{\rm E})\,\hat{\boldsymbol{y}} - \big(u^{\rm S}\partial_z u^{\rm E} + v^{\rm S}\partial_z v^{\rm E}\big)\,\hat{\boldsymbol{z}}\,, \tag{7}$$

where $\hat{\boldsymbol{x}}$ and $\hat{\boldsymbol{y}}$ are unit vectors in horizontal directions.

We simplify the scaling analysis by reusing H and L in (6) for vertical and horizontal near-surface velocity scales. For the x-component of (7) we find

$$\frac{\partial_x \left(\frac{1}{2}\boldsymbol{u}^{\rm S} \cdot \boldsymbol{u}^{\rm S} + \boldsymbol{u}^{\rm S} \cdot \boldsymbol{u}^{\rm E}\right)}{f v^{\rm E}} \sim \frac{\left(\partial_x v^{\rm E} - \partial_y u^{\rm E}\right) v^{\rm S}}{f v^{\rm E}} \sim \frac{U^2/L}{fU} = \mathrm{Ro}\,. \tag{8}$$

A similar result holds for the y-component of (7). Compared to the geostrophic pressure gradient $\partial_z \bar{p} \sim fUL/H$, we find that the vertical component of (7) scales with

$$\frac{u^{\rm S}\partial_z u^{\rm E} + v^{\rm S}\partial_z v^{\rm E}}{\partial_z \bar{p}} \sim \frac{U^2/H}{fUL/H} = \mathrm{Ro}\,. \tag{9}$$

In summary, in nearly geostrophic mesoscale flows, the Stokes–Coriolis term in (2) is $O(1)$ and non-negligible, which means that (2) is a poor approximation to (4) and casts doubt on the Eulerian-mean hypothesis. The other surface wave terms in (2) are $O(\mathrm{Ro})$ and are thus negligible for $\mathrm{Ro} \ll 1$.

2.2 The Lagrangian-mean hypothesis is consistent

The "Lagrangian-mean hypothesis" posits that velocities $\boldsymbol{u}$ that solve (4) are similar to Lagrangian-mean velocities $\boldsymbol{u}^{\rm L}$ that solve (3) at ocean mesoscale and larger. We argue that the Lagrangian-mean hypothesis is consistent with a scaling analysis that suggests the green terms in (3) are negligible at ocean mesoscales and larger.

Using (6) we simplify the surface wave term in (3),

$$(\boldsymbol{\nabla} \times \boldsymbol{u}^{\rm S}) \times \boldsymbol{u}^{\rm L} \approx w^{\rm L}\partial_z u^{\rm S}\,\hat{\boldsymbol{x}} + w^{\rm L}\partial_z v^{\rm S}\,\hat{\boldsymbol{y}} - \big(u^{\rm L}\partial_z u^{\rm S} + v^{\rm L}\partial_z v^{\rm S}\big)\,\hat{\boldsymbol{z}}\,. \tag{10}$$

The term in (10) has the same form as the "non-traditional" component of the Coriolis force associated with the horizontal components of planetary vorticity (which have been neglected *a priori* from (3)). Thus the terms in (10) are small for the same reason we make the traditional approximation for Coriolis forces: because of the dominance of hydrostatic balance, and because geostrophic vertical velocities scale with

$$w^{\mathrm{L}} \sim \mathrm{Ro}\frac{H}{L}U\,, \tag{11}$$

and are therefore miniscule at ocean mesoscales and larger where both Ro and especially H/L are much smaller than unity. Specifically, the same arguments leading to (8) conclude that the horizontal components of (10) scale with Ro^2 — much smaller than $O(1)$ and smaller even than the $O(\mathrm{Ro})$ terms in (8). The vertical component of (10) shares the same scaling with (9): $O(\mathrm{Ro})$ and therefore negligible at ocean mesoscales and larger.

We save the discussion of $\partial_t \boldsymbol{u}^{\mathrm{S}}$ for last. Only the horizontal components of $\boldsymbol{u}^{\mathrm{S}}$ are significant (Vanneste & Young, 2022). $\partial_t \boldsymbol{u}^{\mathrm{S}}$ is primarily associated with wave growth beneath atmospheric storms and thus effectively represents the small part of the total parameterized air-sea momentum transfer that is *depth-distributed* rather than fluxed at or just below the surface (Wagner et al., 2021). We could therefore interpret $\partial_t \boldsymbol{u}^{\mathrm{S}}$ as accounted for implicitly in wave-agnostic models by bulk formulae for air-sea momentum transfer. Even so, we consider a scaling argument by introducing an average $\langle\,\cdot\,\rangle$ over a time-scale T much longer than a day, and therefore much larger than f^{-1}. We find that

$$\frac{\langle \partial_t u^{\mathrm{S}} \rangle}{|f v^{\mathrm{L}}|} \sim \frac{|\boldsymbol{u}^{\mathrm{S}}|}{fT|\boldsymbol{u}^{\mathrm{L}}|} \ll 1\,. \tag{12}$$

We conclude that the Lagrangian-mean hypothesis is consistent since all terms in (3) that explicitly involve surface waves are at least $O(\mathrm{Ro})$ or smaller.

3 Ocean general circulation simulations with and without explicit surface wave effects

We pursue empirical validation of the scaling arguments and conclusions in section 2 by describing a novel wave-averaged general circulation model, and comparing simulated surface velocity fields between a realistic, typical "control" global ocean simulation and a wave-averaged simulation. The comparison shows that typical general circulation models — which do not depend explicitly on the ocean surface wave state — simulate and output Lagrangian-mean currents. Both the control and wave-averaged general circulation simulations use models based on the Modular Ocean Model 6 (MOM6) following the Geophysical Fluid Dynamics Laboratory (GFDL)'s OM4 configuration (Adcroft et al., 2019).

3.1 Control general circulation model based on MOM6

Our control MOM6-based general circulation model (GCM) is called "Ocean Model 4", or OM4. OM4 is a typical GCM that discretizes and time-integrates the horizontal components of the wave-agnostic, implicitly-averaged Boussinesq momentum equation (4), with hydrostatic balance

$$\partial_z p = b\,, \tag{13}$$

approximating the vertical component of (4).

3.2 A wave-averaged MOM6

Our wave-averaged GCM, dubbed "OM4-CL" (CL after Craik & Leibovich, 1976) discretizes and time-integrates the horizontal components of the wave-averaged Craik–Leibovich Boussinesq momentum equation (3). OM4-CL replaces the vertical component of equation (3) with "wavy hydrostatic balance" (Suzuki & Fox-Kemper, 2016)

$$\partial_z \bar{p} = \bar{b} - (u^{\mathrm{L}}\partial_z u^{\mathrm{S}} + v^{\mathrm{L}}\partial_z v^{\mathrm{S}})\,. \tag{14}$$

In OM4-CL, tracers are advected by $\boldsymbol{u}^{\mathrm{L}}$. Mass conservation is enforced by requiring that $\boldsymbol{u}^{\mathrm{L}}$ is divergence-free, which Vanneste and Young (2022) show is a valid approximation in the CL equations. OM4-CL follows advances of many previous works on the averaged effects of surface waves on ocean circulation (McWilliams & Restrepo, 1999; Suzuki & Fox-Kemper, 2016; Couvelard et al., 2020) to implement the wave-averaged equations in an ocean general circulation model. However, OM4-CL is unique in simulating the Lagrangian-mean velocity directly. Simulating the Lagrangian-mean velocity is mathematically equivalent to simulating the Eulerian-mean velocity, but simplifies the model implementation due to the structural similarities between (3) and (4) (as will be described in detail in a forthcoming documentation paper).

3.3 Coupled sea ice–ocean model simulations

Both the control OM4 and the wave-averaged OM4-CL simulations follow the approach for coupled ocean and sea-ice model initialization and forcing laid out by Adcroft et al. (2019). Prescribed atmospheric and land forcing fields in these simulations are obtained from the JRA55-do reanalysis product (Tsujino et al., 2018), following recommendations from the second Ocean Model Intercomparison Project protocol (OMIP2, see Griffies et al., 2016; Tsujino et al., 2020). Simulations are performed with a nominal lateral resolution of $1/4^{\circ}$ that partially resolves mesoscale eddies. Our configuration is similar to OM4p25 described by Adcroft et al. (2019), including a hybrid vertical coordinate with two meter vertical resolution near the surface that transitions to isopycnal coordinates in the ocean interior. Both OM4 and OM4-CL use the same wave-dependent surface boundary layer vertical mixing parameterization (Reichl & Li, 2019) with the same modeled Stokes drift input. We conduct simulations using forcing from 1958-2017 and analyze model output from the last 20 years (1998-2017).

For the wave-averaged simulations, global Stokes drift velocities are taken from an offline WAVEWATCH-III v6.07 simulation (The WAVEWATCH III Development Group (WW3DG), 2016), following a similar procedure to Li et al. (2019); Reichl and Deike (2020). The Stokes drift profile is reconstructed from five exponentially-decaying surface Stokes drift wavenumber bands (equation (9) in Li et al., 2019), which closely matches the profile of Stokes drift obtained from the full wavenumber spectrum (here simulated using 25 discrete wavenumber bands). The wave model has a horizontal resolution of about 50km, is forced with the same JRA55-do wind product as the ocean, and includes simulated sea-ice provided from the standard OM4 configuration. For simplicity we neglect the feedback effects of ocean currents on advecting and refracting waves, which are not expected to qualitatively effect our conclusions due to the coarse model scales used in these experiments.

Note that the same winds — not the same wind stress — force both OM4 and OM4-CL, and that OM4-CL includes the Stokes tendency term $\partial_t \boldsymbol{u}^{\mathrm{S}}$ in equation (3). As a result, OM4 and OM4-CL have slightly different column-integrated momentum budgets (Fan et al., 2009; Wagner et al., 2021). Nevertheless, figures 2 and 3 show that these discrepancies are not important.

3.4 A conspicuous correlation between instantaneous wave-agnostic and Lagrangian-mean currents

Figure 1 compares daily-averaged surface currents in OM4 and OM4CL. Figure 1c shows that the difference between OM4 and OM4-CL surface currents is noisy, which we attribute to chaotic mesoscale variability. But the difference between OM4 surface currents and *Eulerian-mean* surface currents from OM4-CL, plotted in figure 1d, nevertheless exhibits a large-scale signal amidst the mesoscale noise suspiciously similar to the Stokes drift in figure 1e.

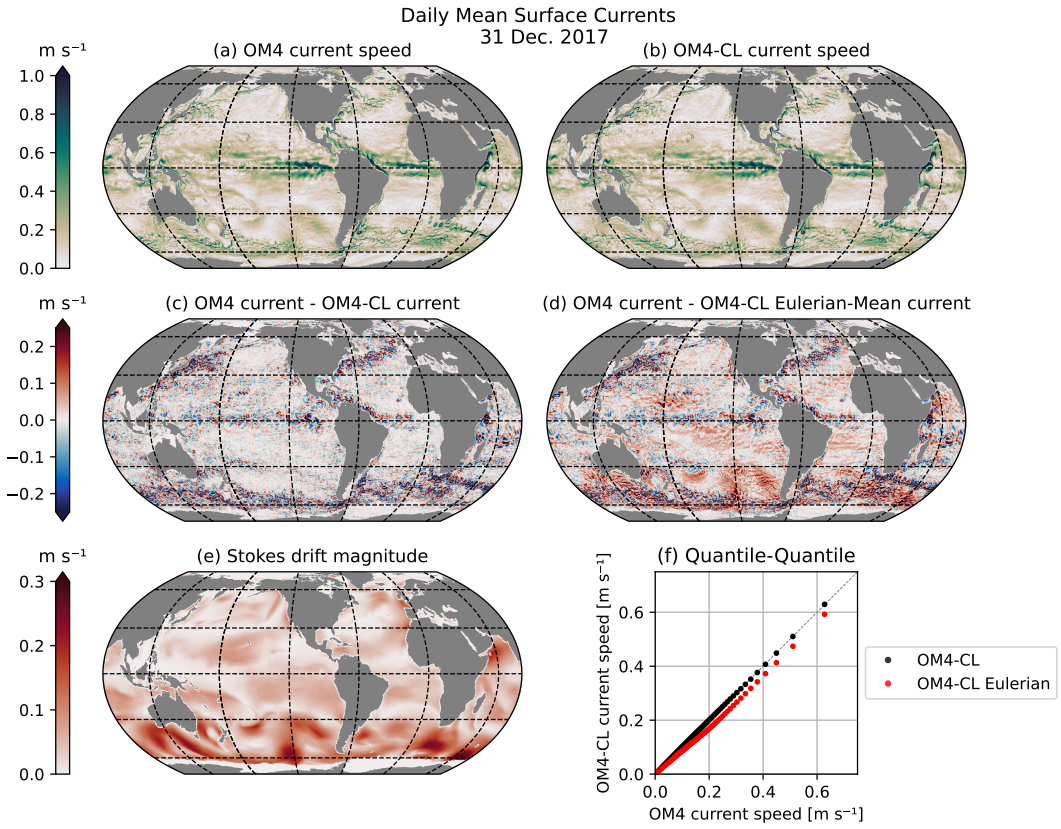

Figure 1: Comparison of daily-mean snapshot of surface currents in OM4 and OM4-CL. (a) surface current speed in OM4. (b) surface current speed in OM4-CL. (c) Difference of the surface current speed in OM4 (panel (a)) and OM4-CL (panel (b)). (d) Difference of the surface current speed in OM4 (panel (a)) and the Eulerian mean current from OM4-CL. (e) Stokes drift current magnitude. (f) The comparison of the quantile–quantile plot for surface current speeds between *(i)* OM4-CL and OM4 and *(ii)* Eulerian mean OM4-CL and OM4. The signature of Stokes drift surface current (e) is evident in panel (d).

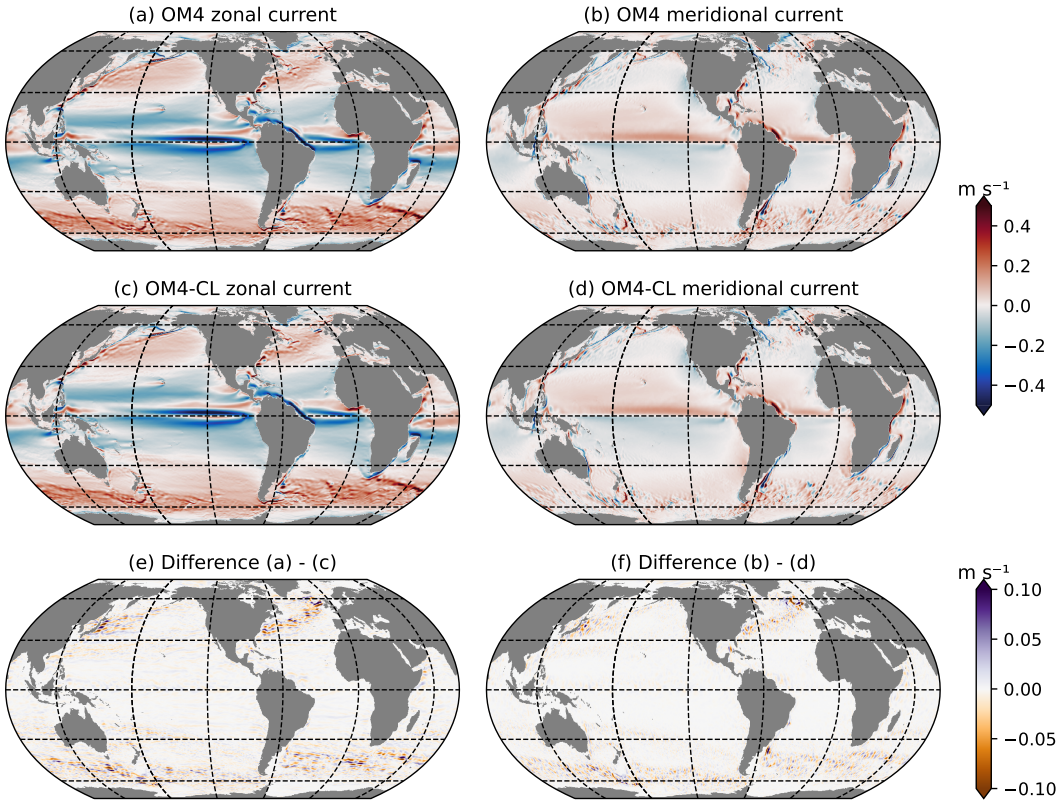

Figure 2: (Upper) OM4 zonal and meridional surface currents ($\boldsymbol{u}$ in (4)) averaged between 1998-2017, (middle) time-averaged OM4-CL zonal and meridional currents ($\boldsymbol{u}^{\mathrm{L}}$ in (3)), and (bottom) differences between the upper two rows. Note the different color scales between panels (a)-(d) and the bottom two panels.

To quantify this large-scale discrepancy, we plot correlation of the corresponding quantiles in figure 1f. Figure 1f demonstrates that the OM4 surface current is perfectly correlated with the Lagrangian-mean current of OM4-CL, while betraying a systematic mismatch between OM4-CL's Eulerian-mean current, validating the Lagrangian-mean hypothesis for OM4. To eliminate the differences in surface currents due to mesoscale eddy variability, we investigate multi-decadal time-averages of the surface currents in OM4 and OM4-CL.

3.5 Time-averaged wave-agnostic currents are almost identical to time-averaged Lagrangian-mean currents

Figure 2 compares surface currents between the control OM4 and the wave-averaged OM4-CL. OM4 simulates "implicitly-averaged" currents with no explicit surface wave dependence, while OM4-CL explicitly simulates Lagrangian-mean surface currents. Currents output from both OM4 and OM4-CL are further averaged over the time period 1998-2017. The similarity of figure 2a-b, which show zonal and meridional components of $\boldsymbol{u}$ from OM4, and figure 2c-d, which show the zonal and meridional components of the Lagrangian-mean $\boldsymbol{u}^{\mathrm{L}}$ from OM4-CL, demonstrate that the surface circulation in OM4 and the Lagrangian-mean surface circulation in OM4-CL are almost identical. The differences between the zonal and meridional components of $\boldsymbol{u}$ and $\boldsymbol{u}^{\mathrm{L}}$, shown in the bottom row of figure 2, are small and associated with chaotic mesoscale perturbations.

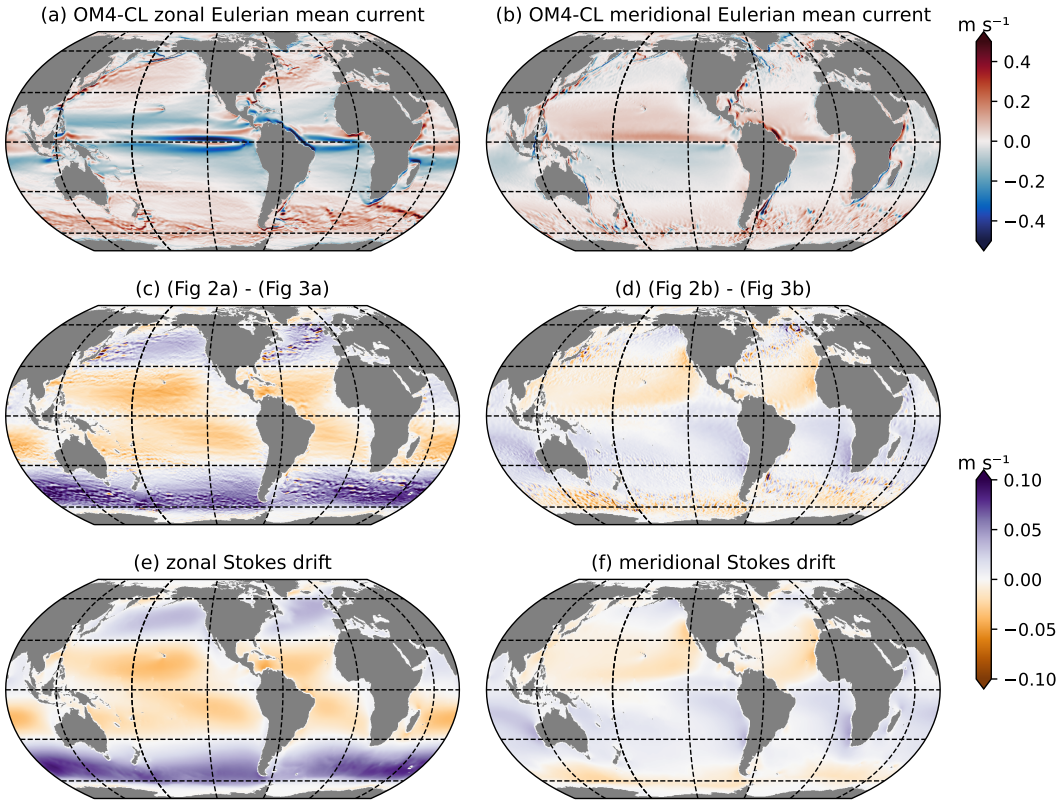

Figure 3: (Upper) Mean OM4-CL zonal and meridional Eulerian-mean surface currents (1998-2017), (middle) difference between OM4-CL Eulerian mean currents and OM4 currents, and (bottom) mean surface Stokes drift.

Finally, we directly evaluate the Eulerian-mean hypothesis within OM4 and OM4-CL. The Eulerian-mean velocity is calculated from OM4-CL output by subtracting the Stokes drift from the simulated velocity $\boldsymbol{u}^{\mathrm{L}}$ according to (1). The Eulerian-mean hypothesis posits that the mean velocity in the control OM4 simulation is close or identical to Eulerian-mean velocity from the OM4-CL simulation. However, the middle row of figure 3 reveals a systematic and significant difference between the Eulerian-mean velocity from OM4-CL and the wave-agnostic velocity from OM4 which is much larger than the differences exhibited in the bottom row of figure 2. Furthermore, the difference between the currents from the control simulation and the Eulerian-mean currents from the wave-averaged simulation (middle row of figure 3) turns out to be almost identical to the mean surface Stokes drift currents (bottom row of figure 3). We thus do not find evidence to support the Eulerian-mean hypothesis. Instead, the current simulated by the wave-agnostic OM4 is close to the Lagrangian-mean current simulated by OM4-CL, as predicted by the Lagrangian-mean hypothesis.

4 Discussion

By inspecting the wave-averaged equations of motion, and comparing the output from wave-neglecting control simulation and an explicitly wave-averaged simulation, we come to three conclusions. First, the Eulerian-mean hypothesis does not encapsulate a consistent theoretical argument, and therefore Stokes drift should not be added to general circulation model output. Second, ocean GCMs with horizontal resolutions of 1/4° and coarser (and thus with geostrophically-balanced velocities) may accurately simulate the surface-wave-averaged

Lagrangian-mean velocity. Finally, resolved — not parameterized — surface wave effects are negligible at large oceanic scales where Coriolis forces dominate.

We note that the Eulerian-mean hypothesis assumes the Eulerian-mean velocity field is "fundamental", and that the Lagrangian-mean velocity is a diagnostic quantity that can be computed by combining the Eulerian-mean velocity obtained from a dynamical balance and a Stokes drift velocity diagnosed from the surface wave field. Our results advance a different paradigm: the Lagrangian-mean velocity is the fundamental mean quantity to be determined from the mean momentum balance, while the Eulerian-mean velocity is diagnostic, and "dependent" on the surface wave field. The fundamental nature of the Lagrangian-mean or "total" momentum balance is also emphasized by Samelson (2022) using averages in a surface-following coordinate system similar to the Lagrangian-mean.

4.1 Boundary layer parameterization in general circulation models

General circulation models that solve the Lagrangian-mean equations use — explicit or implicitly — parameterizations formulated in terms of $\boldsymbol{u}^{\mathrm{L}}$. For example, both OM4 (Reichl & Li, 2019) and the K-profile parameterization (Large et al., 1994) model the turbulent vertical flux of horizontal momentum with

$$\boldsymbol{\mathcal{X}} \approx \partial_z \left(K \, \partial_z \boldsymbol{u}^{\mathrm{L}} \right) , \tag{15}$$

where the turbulent vertical diffusivity K is a nonlinear function of mean buoyancy $\bar{b}$, mean velocity $\boldsymbol{u}^{\mathrm{L}}$, surface boundary conditions, and depth z. We emphasize that the parameterization in equation (15) is sensible, as it dissipates mean kinetic energy $\frac{1}{2}|\boldsymbol{u}^{\mathrm{L}}|^2$ (Wagner et al., 2021) and is consistent with large eddy simulation results. For example, Reichl et al. (2016) find momentum fluxes aligned with $\partial_z \boldsymbol{u}^{\mathrm{L}}$ in large eddy simulations of hurricane-forced boundary layer turbulence, and Pearson (2018) observe that turbulent mixing beneath surface waves tends to homogenize $\boldsymbol{u}^{\mathrm{L}}$.

4.2 Future applications of wave-averaged general circulation models

Figures 2 and 3 show that resolved surface wave effects are negligible at $1/4^\circ$ degree resolution. However, we expect that resolved surface wave effects become more relevant at finer resolutions and higher Rossby numbers, when the term $\left(\boldsymbol{\nabla} \times \boldsymbol{u}^{\mathrm{S}}\right) \times \boldsymbol{u}^{\mathrm{L}}$ in (3) is no longer negligible. The question remains: "At what resolution do wave effects matter for mesoscale or submesoscale dynamics?" Surface wave effects are known to be important at the $O(1\,\mathrm{m})$ scales of ocean surface boundary layer large eddy simulations (McWilliams et al., 1997), but the effects of surface wave on motions with scales between $O(1\,\mathrm{m})$ and $1/4^\circ$ remains relatively unexplored (Hypolite et al., 2021; Suzuki et al., 2016).

Even $1/4^\circ$-resolution GCMs benefit from knowledge of the surface wave state when their boundary layer turbulence parameterizations depend on the surface wave state (Li et al., 2019). This is also true for air-sea flux parameterizations (Reichl & Deike, 2020) and potentially other parameterizations, such as those for wave-ice interaction.

Open Research

The MOM6 source code including modifications for MOM6-CL is available at `https://github.com/mom-ocean/MOM6`. WAVEWATCH III source code is available from `https://github.com/NOAA-EMC/WW3`. Code and model output used for generating figures are available at `https://github.com/breichl/MOM6CL-Figures` (and will be linked to Zenodo upon acceptance).

Acknowledgments
Without implying endorsement, we gratefully acknowledge discussions and even material

assistance from Alistair Adcroft, Brandon Allen, Keaton Burns, Raffaele Ferrari, Glenn Flierl, Baylor Fox-Kemper, Stephen Griffies, Andy Hogg, Adele Morrison, Callum Shakespeare, William Young, and many others — not least of all the late Sean Haney. Be careful, Sean. G.L.W. is supported by the generosity of Eric and Wendy Schmidt by recommendation of the Schmidt Futures program, and by the National Science Foundation under grant AGS-6939393. N.C.C. is supported by the Australian Research Council DECRA Fellowship DE210100749. We extend additional thanks to Zoom Video Communications for allowing collaboration during the difficult times of the COVID-19 pandemic.

References

Adcroft, A., Anderson, W., Balaji, V., Blanton, C., Bushuk, M., Dufour, C. O., ... Zhang, R. (2019). The GFDL global ocean and sea ice model OM4.0: Model description and simulation features. *J. Adv. Model Earth Sy.*. doi: 10.1029/2019MS001726

Bosi, S., Broström, G., & Roquet, F. (2021). The role of Stokes drift in the dispersal of North Atlantic surface marine debris. *Frontiers in Marine Science*, *8*, 697430. doi: 10.3389/fmars.2021.697430

Bühler, O. (2014). *Waves and mean flows*. Cambridge University Press.

Chassignet, E. P., Xu, X., & Zavala-Romero, O. (2021). Tracking marine litter with a global ocean model: Where does it go? Where does it come from? *Frontiers in Marine Science*, *8*, 697430. doi: 10.3389/fmars.2021.667591

Couvelard, X., Lemarié, F., Samson, G., Redelsperger, J.-L., Ardhuin, F., Benshila, R., & Madec, G. (2020). Development of a two-way-coupled ocean–wave model: assessment on a global NEMO (v3. 6)–WW3 (v6. 02) coupled configuration. *Geoscientific Model Development*, *13*(7), 3067–3090.

Craik, A. D. D., & Leibovich, S. (1976). A rational model for Langmuir circulations. *Journal of Fluid Mechanics*, *73*(3), 401–426.

Cunningham, H. J., Higgins, C., & van den Bremer, T. S. (2022). The role of the unsteady surface wave-driven Ekman–Stokes flow in the accumulation of floating marine litter. *Journal of Geophysical Research: Oceans*, *127*(6), e2021JC018106.

Dobler, D., Huck, T., Maes, C., Grima, N., Blanke, B., Martinez, E., & Ardhuin, F. (2019). Large impact of Stokes drift on the fate of surface floating debris in the South Indian basin. *Marine Pollution Bulletin*, *148*, 202–209.

Durgadoo, J. V., Biastoch, A., New, A. L., Rühs, S., Nurser, A. J., Drillet, Y., & Bidlot, J.-R. (2021). Strategies for simulating the drift of marine debris. *Journal of Operational Oceanography*, *14*(1), 1–12.

Fan, Y., Ginis, I., & Hara, T. (2009). The effect of wind–wave–current interaction on air–sea momentum fluxes and ocean response in tropical cyclones. *Journal of Physical Oceanography*, *39*(4), 1019–1034.

Fraser, C. I., Morrison, A. K., Hogg, A. M., Macaya, E. C., van Sebille, E., Ryan, P. G., ... Waters, J. M. (2018). Antarctica's ecological isolation will be broken by storm-driven dispersal and warming. *Nature Climate Change*, *8*(8), 704–708.

Griffies, S. M., Danabasoglu, G., Durack, P. J., Adcroft, A. J., Balaji, V., Böning, C. W., ... Yeager, S. (2016). OMIP contribution to CMIP6: experimental and diagnostic protocol for the physical component of the Ocean Model Intercomparison Project. *Geoscientific Model Development*, *9*, 3231–3296. doi: 10.5194/gmd-9-3231-2016

Herman, A., & Węsławski, J. M. (2022). Typical and anomalous pathways of surface-floating material in the northern North Atlantic and Arctic Ocean. *Scientific Reports*, *12*(1), 1–13. doi: 10.1038/s41598-022-25008-5

Huang, N. E. (1979). On surface drift currents in the ocean. *Journal of Fluid Mechanics*, *91*(1), 191–208.

Hypolite, D., Romero, L., McWilliams, J. C., & Dauhajre, D. P. (2021). Surface gravity wave effects on submesoscale currents in the open ocean. *Journal of Physical Oceanography*, *51*(11), 3365–3383.

Iwasaki, S., Isobe, A., Kako, S., Uchida, K., & Tokai, T. (2017). Fate of microplastics and

mesoplastics carried by surface currents and wind waves: A numerical model approach in the Sea of Japan. *Marine Pollution Bulletin*, *121*(1-2), 85–96.

Johannessen, J., Chapron, B., Collard, F., Rio, M., Piollé, J., Gaultier, L., ... others (2016). GlobCurrent: Multisensor synergy for surface current estimation..

Kafiabad, H. A., Vanneste, J., & Young, W. R. (2021). Wave-averaged balance: a simple example. *Journal of Fluid Mechanics*, *911*, R1.

Kerpen, N. B., Schlurmann, T., Schendel, A., Gundlach, J., Marquard, D., & Hüpgen, M. (2020). Wave-induced distribution of microplastic in the surf zone. *Frontiers in Marine Science*, *7*, 590565.

Kubota, M. (1994). A mechanism for the accumulation of floating marine debris north of Hawaii. *Journal of Physical Oceanography*, *24*(5), 1059–1064.

Large, W. G., McWilliams, J. C., & Doney, S. C. (1994). Oceanic vertical mixing: A review and a model with a nonlocal boundary layer parameterization. *Reviews of Geophysics*, *32*(4), 363–403.

Li, Q., Reichl, B. G., Fox-Kemper, B., Adcroft, A. J., Belcher, S. E., Danabasoglu, G., ... Zheng, Z. (2019). Comparing ocean surface boundary vertical mixing schemes including Langmuir turbulence. *Journal of Advances in Modeling Earth Systems*, *11*(11), 3545-3592. doi: 10.1029/2019MS001810

Longuet-Higgins, M. (1969). On the transport of mass by time-varying ocean currents. In *Deep Sea Research and Oceanographic Abstracts* (Vol. 16, pp. 431–447).

McWilliams, J. C., & Restrepo, J. M. (1999). The wave-driven ocean circulation. *Journal of Physical Oceanography*, *29*(10), 2523–2540.

McWilliams, J. C., Sullivan, P. P., & Moeng, C.-H. (1997). Langmuir turbulence in the ocean. *Journal of Fluid Mechanics*, *334*, 1–30.

Middleton, J. F., & Loder, J. W. (1989). Skew fluxes in polarized wave fields. *Journal of Physical Oceanography*, *19*(1), 68–76. doi: 10.1175/1520-0485(1989)019<0068:SFIPWF>2.0.CO;2

Onink, V., Kaandorp, M. L. A., van Sebille, E., & Laufkötter, C. (2022). Influence of particle size and fragmentation on large-scale microplastic transport in the Mediterranean Sea. *Environmental Science & Technology*, *0*(0), null. doi: 10.1021/acs.est.2c03363

Onink, V., Wichmann, D., Delandmeter, P., & Van Sebille, E. (2019). The role of Ekman currents, geostrophy, and Stokes drift in the accumulation of floating microplastic. *Journal of Geophysical Research: Oceans*, *124*(3), 1474–1490.

Pearson, B. (2018). Turbulence-induced anti-Stokes flow and the resulting limitations of large-eddy simulation. *Journal of Physical Oceanography*, *48*(1), 117–122.

Reichl, B. G., & Deike, L. (2020). Contribution of sea-state dependent bubbles to air-sea carbon dioxide fluxes. *Geophysical Research Letters*, *47*(9), e2020GL087267. doi: 10.1029/2020GL087267

Reichl, B. G., & Li, Q. (2019). A parameterization with a constrained potential energy conversion rate of vertical mixing due to Langmuir turbulence. *Journal of Physical Oceanography*, *49*(11), 2935–2959.

Reichl, B. G., Wang, D., Hara, T., Ginis, I., & Kukulka, T. (2016). Langmuir turbulence parameterization in tropical cyclone conditions. *Journal of Physical Oceanography*, *46*(3), 863–886.

Samelson, R. (2022). Wind drift in a homogeneous equilibrium sea. *Journal of Physical Oceanography*, *52*(9), 1945–1967.

Skyllingstad, E. D., & Denbo, D. W. (1995). An ocean large-eddy simulation of Langmuir circulations and convection in the surface mixed layer. *Journal of Geophysical Research: Oceans*, *100*(C5), 8501–8522.

Smith, J. A. (2006). Observed variability of ocean wave Stokes drift, and the Eulerian response to passing groups. *Journal of Physical Oceanography*, *36*(7), 1381–1402. doi: 10.1175/JPO2910.1

Stokes, G. G. (1847). On the theory of oscillatory waves. *Trans. Camb. Phil. Soc.*, *8*, 411–455.

Sullivan, P. P., & McWilliams, J. C. (2010). Dynamics of winds and currents coupled to surface waves. *Annual Review of Fluid Mechanics*, *42*, 19–42.

Suzuki, N., & Fox-Kemper, B. (2016). Understanding Stokes forces in the wave-averaged equations. *Journal of Geophysical Research: Oceans*, *121*(5), 3579–3596.

Suzuki, N., Fox-Kemper, B., Hamlington, P. E., & Van Roekel, L. P. (2016). Surface waves affect frontogenesis. *Journal of Geophysical Research: Oceans*, *121*(5), 3597–3624.

Tamura, H., Miyazawa, Y., & Oey, L.-Y. (2012). The Stokes drift and wave induced-mass flux in the North Pacific. *Journal of Geophysical Research: Oceans*, *117*(C8).

The WAVEWATCH III Development Group (WW3DG). (2016). *User manual and system documentation of WAVEWATCH III version 5.16.* (Tech. Rep. No. 329). NOAA/NWS/NCEP/MMAB.

Tsujino, H., Urakawa, L. S., Griffies, S. M., Danabasoglu, G., Adcroft, A. J., Amaral, A. E., ... Yu, Z. (2020). Evaluation of global ocean–sea-ice model simulations based on the experimental protocols of the Ocean Model Intercomparison Project phase 2 (OMIP-2). *Geoscientific Model Development*, *13*(8), 3643–3708. doi: 10.5194/gmd-13-3643-2020

Tsujino, H., Urakawa, S., Nakano, H., Small, R. J., Kim, W. M., Yeager, S. G., ... Yamazaki, D. (2018). JRA-55 based surface dataset for driving ocean - sea-ice models (JRA55-do). *Ocean Modelling*, *130*, 79–139.

Van den Bremer, T. S., & Breivik, Ø. (2017). Stokes drift. *Philosophical Transactions of the Royal Society A: Mathematical, Physical and Engineering Sciences*, *376*(2111), 20170104.

Vanneste, J., & Young, W. R. (2022). Stokes drift and its discontents. *Philosophical Transactions of the Royal Society A*, *380*(2225), 20210032.

Van Sebille, E., Aliani, S., Law, K. L., Maximenko, N., Alsina, J. M., Bagaev, A., ... others (2020). The physical oceanography of the transport of floating marine debris. *Environmental Research Letters*, *15*(2), 023003.

Van Sebille, E., Zettler, E., Wienders, N., Amaral-Zettler, L., Elipot, S., & Lumpkin, R. (2021). Dispersion of surface drifters in the tropical Atlantic. *Frontiers in Marine Science*, *7*, 607426.

Wagner, G. L., Chini, G. P., Ramadhan, A., Gallet, B., & Ferrari, R. (2021). Near-inertial waves and turbulence driven by the growth of swell. *Journal of Physical Oceanography*, *51*(5), 1337–1351.

Wagner, G. L., & Young, W. R. (2015). Available potential vorticity and wave-averaged quasi-geostrophic flow. *Journal of Fluid Mechanics*, *785*, 401–424.